ELSEVIER

Micro and nano-fabrication of biodegradable polymers for drug delivery

Y. Lu, S.C. Chen*

Department of Mechanical Engineering, The University of Texas at Austin, 1 University Station, C2200, Austin TX, 78712, USA

Abstract

This paper presents state-of-the-art micro and nano-fabrication techniques for biodegradable polymers. Replication molding, using a rigid or elastic master, can pattern structures on a polymer surface in a submicron resolution at a low cost. Layer-by-layer rapid prototyping methods are promising in producing controlled release units with complicated geometries, release mechanisms and the ability to control microstructure and composition. Special attention is paid to the fast, flexible, and non-invasive laser fabrication techniques that have great potential in the fabrication of biodegradable polymer drug delivery devices in both a laboratory and industry scale.
© 2004 Elsevier B.V. All rights reserved.

Contents

* Corresponding author. Tel.: +1-512-232-6094; fax: +1-512-471-1045.
E-mail address: scchen@mail.utexas.edu (S.C. Chen).

1. Introduction

The advances in micro- and nano-fabrication technology have enhanced the tools available to create clinically important therapeutic applications. Microfabrication technology has been applied to the successful fabrication of a variety of implantable and oral drug delivery devices based on silicon, glass, silicone elastomer, or plastic materials [1–5]. Such devices would permanently remain in the biological tissue if not removed surgically. Because of the inherent difficulty in retrieving small-scale devices from tissues, it is advantageous to apply biodegradable polymers that would naturally degrade and disappear in tissue over a desired period of time. Biodegradable polymer conduits and tissue engineering scaffolds were produced using extrusion [6], fiber bonding [7], salt leaching, and laminating [8]. However, micro and nano-fabrication of biodegradable polymers with precise control over surface microarchitecture, topography, and size remains an important challenge. Traditionally, silicon-based microelectromechanical systems (MEMS) are fabricated by the repeated application of unit process steps such as thin-film deposition, photolithography, and etching. Unfortunately, these methods are not suitable for biodegradable polymers. Significant effort has been devoted to develop novel micro and nanofabrication techniques for biodegradable polymers in

the recent years. This paper will review some of the current approaches targeting drug delivery devices.

2. Biodegradable polymers

Over the past decade the use of biodegradable polymers for the administration of pharmaceuticals and biomedical devices has increased dramatically. The most important biomedical applications of biodegradable polymers are in the areas of controlled drug delivery systems [9], in the forms of implants and devices for bone and dental repairs [10,11].

Biodegradable polymers can be either natural or synthetic. In general, synthetic polymers offer greater advantages than natural ones in that they can be tailored to give a wider range of properties [12]. The general criteria for selecting a polymer for use as a degradable biomaterial are to match the mechanical properties and the degradation rate to the needs of the application. Commonly used biodegradable polymers, along with their selected physical and chemical characteristics, are listed in Table 1. Poly(D-lactic acid) (PDLA) is a biodegradable polymer with extensive medical applications due to its biodegradable property that has been proven harmless to human body cells. PDLA has been used as a substrate material for potential applications in nerve regeneration in the field of tissue engineering. Poly(ε-capro-

Table 1
List of some biodegradable polymers for biomedical applications

Polymer	T_m (°C)	T_g (°C)	Tensile modulus (MPa)	Degradation time (months)
Polyglycolic acid	225–230	35–40	7	6–12
L-Polylactic acid	173–178	60–65	2.7	>24
DL-Polylactic acid	Amorphous	55–60	1.9	12–16
Polycaprolactone	58–63	(−65)–(−60)	0.4	>24
85/15 poly(DL-lactide-*co*-glycolide)	Amorphous	50–55	2.0	5–6

lactone) (PCL), an aliphatic polyester, is one of the most important biodegradable polymers in medicine. Some of the applications of PCL are sutures and biocompatible medical devices. Poly(vinyl alcohol) (PVA) is used in a wide range of applications such as adhesives, fibers, textile, paper-sizing, and water-soluble packaging. It is also used to modify the degradation profile of other polymers [13–15]. These polymers have unique features such as controllability of mechanical properties, tailoring of degradation rates, and minimal toxicity and immune response that make them ideal for medical uses. In the following sections, we will present several micro and nanofabrication techniques developed for biodegradable polymers.

3. Replication techniques

Replication technologies are proven useful for biodegradable polymer microfabrication because the principles behind these processes are straightforward and well known in the macroworld. The underlying principle is the replication of a microfabricated mold tool, which represents the inverse geometry of the desired polymer structure. The expensive microfabrication step is only necessary for the initial fabrication of this master structure, which then can be replicated many times into the polymer substrate. In addition to the cost advantage, replication techniques also offer the benefit of the freedom of design: the master can be fabricated with a large number of different microfabrication technologies, which allow various geometries to be realized.

3.1. Microimprinting lithography

Also known as "hot embossing" or "compression molding", microimprinting lithography is one of the most widely used processes to fabricate microstructures for data storage, wave gratings, or microfluidic applications [13,16–18]. In hot embossing, a master with a micro-scale relief structure on the surface was first fabricated by standard integrated circuit techniques. A chrome lithographic mask was produced on a quartz wafer with the desired micropatterns using e-beam lithography. The quartz substrate was etched using reactive ion etching (RIE) through the mask,

leaving areas covered by chrome. After removing the chrome, the quartz substrate was silanized by exposure to the vapor of $CF_3(CF_2)_6(CH_2)_2SiCl_3$ for ~ 30 min. We used this mold as a micro die to transfer the geometric micropatterns to the biodegradable polymer.

PCL films were obtained by casting a PCL chloroform solution (80% w/v) onto a glass wafer. They were then placed on the quartz die and heated between two plates just below the melting temperature T_m, which was 57 °C. A vacuum was applied to prevent the formation of air bubbles due to entrapped air. A 500 psi (3.4 MPa) pressure was placed between two plates for 10 min. Temperature was gradually lowered to release internal stress from the crystallization and different thermal expansion coefficients of the master and the polymer film. The resulting PCL film with a surface pattern was peeled off easily. The geometry was inversed to the one of the quartz mold, while the corners were rounded and the walls were slightly distorted (Fig. 1A). Adhesion between the mold and the polymer was minimized by the carbon fluoride surface coating. The pattern distortion was due to the remaining internal stress built up at the corners and to the lack of robustness of the material itself. This fast, relatively inexpensive technique is capable of patterning nano-scale features on a planar surface. However, it requires the thermoplastic polymer to have a good thermal stability near the glass transition temperature T_g.

3.2. Soft lithography

Softlithography is a general term of several nonphotolithographic techniques based on self-assembly and replica molding for micro and nano-fabrication. In soft lithography, an elastomeric stamp with patterned relief structures on its surface is used to generate patterns and structures with feature sizes ranging from 30 nm to 100 μm. This convenient, effective, and low-cost method has been widely used in micro/nanofabrication, particularly, in biomaterial fabrications [19,20]. Xia and Whitesides [21] had a detailed review on softlithographic techniques.

The essential element of this technique is the elastomeric stamp prepared by cast molding a crosslinkable elastomer over a master with surface relief structures. A quartz master was fabricated using e-beam lithography and RIE, as introduced in the
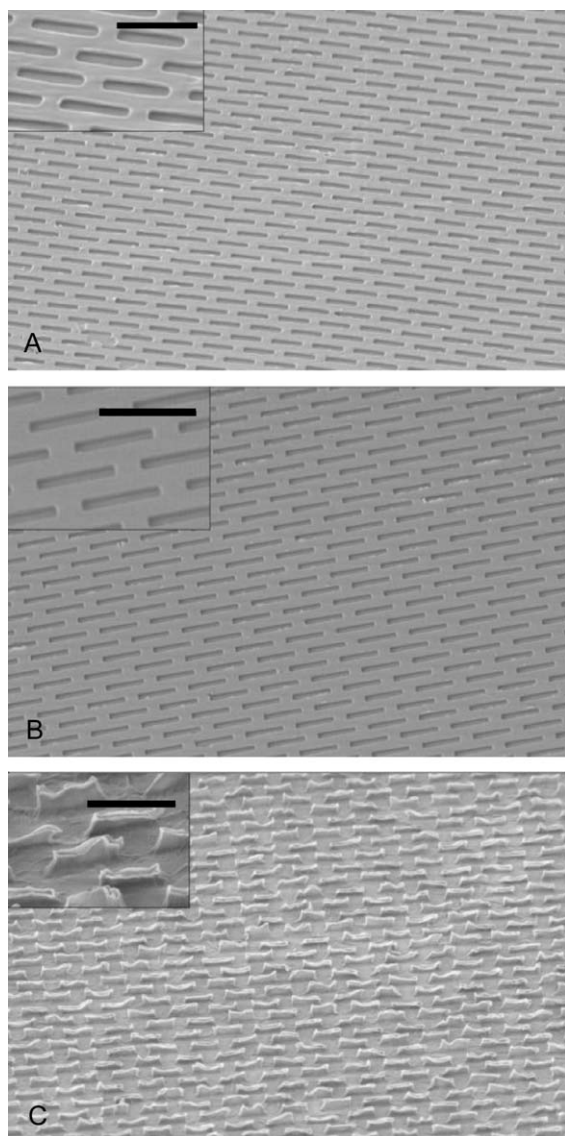
Fig. 1. (A) Hot embossed microfeature in PCL; (B) PDMS stamp; (C) PCL film with surface relief structures fabricated by solvent-assisted molding. Scale bars in 5 μm.

previous subject. Alternatively, a master can also be produced using standard photolithographic processes on an SU-8 photoresist. A Poly(dimethylsiloxane) (PDMS) elastomer (Sylgard™ 184) kit including a liquid silicone rubber base and a curing agent was mixed and poured over the quartz master. The liquid was heated and solidified at 70 °C within a few hours

via hydrosilylation reaction. The PDMS stamp was ready to use after it was peeled off (Fig. 1B).

We used solvent-assisted molding as a demonstration of soft lithographic techniques. A drop of PCL solution in chloroform (80% w/v) was placed on a glass wafer. The PDMS stamp was then applied to the liquid against the wafer with little force. The solvent was evaporated at room temperature for 24 h before the PCL film formed and was peeled off from the stamp. The PCL film had a surface relief structure conformal to the structure on the quartz master, despite imperfections caused by adhesion between PCL and the PDMS stamp can be seen (Fig. 1C).

4. Rapid prototyping techniques

Rapid prototyping techniques have been applied to manufacturing components with complex geometries beyond the reach of conventional precise machining. The fabrication process is directed by computer-aid design (CAD) of a certain component. Methods including direct deposition [22–24], selective laser sintering [25], three-dimensional printing [26], and stereolithography [27–29] have been developed recently, which build components in a laminated fashion.

4.1. Direct deposition methods

Direct deposition microfabrication techniques, which are essentially micro-scale extrusion, were solely derived from their macrofabrication counterpart [22]. A pressure-assisted microsyringe method was used to create a poly(lactic-co-glycolic) acid (PLGA) scaffold with micro-scale porosity [23]. A solution of PLGA in a volatile solvent was placed inside a syringe and expelled through a 10-μm needle. The syringe was mounted on the z-axis of a three-axis micropositioning system. The lateral resolution of the deposited structure ranged up to 5 μm, depending on the process parameters. Similarly, PCL scaffolds were fabricated using the micro-extrusion of PCL filaments under several MPa, resulting in a resolution of several hundred microns [24]. 3D scaffolds can be made by stacking 2D layers in both techniques. However, the geometry is limited since the upper layer has to be supported by the lower one.
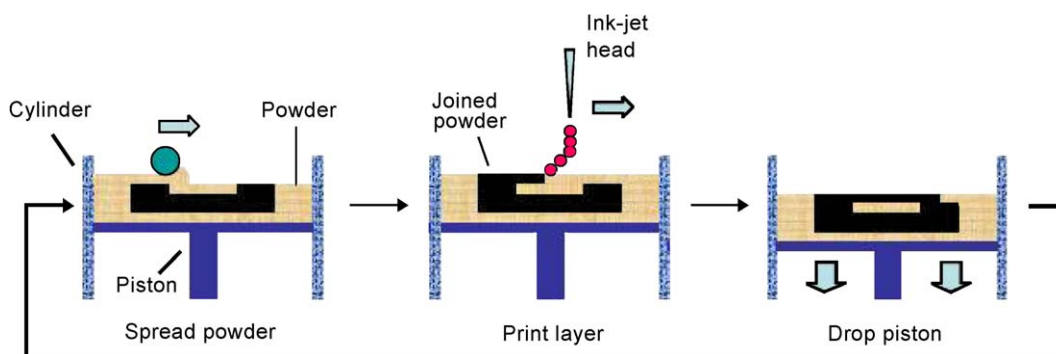
Fig. 2. Schematic operation of three-dimensional printing.

4.2. Three-dimensional printing

Three-dimensional printing has demonstrated the capability of fabricating microstructures and controlling local composition with a high resolution in the interior of the component [26]. From a computer model (CAD) of the desired part, a slicing algorithm draws detailed information for every layer. Each layer begins with a thin distribution of powder spread over the surface of a powder bed. Using a technology similar to ink-jet printing, a binder material selectively joins particles where the object is to be formed. A piston that supports the powder bed and the part-in-progress lowers so that the next powder layer can be spread and selectively joined. This layer-by-layer process repeats until the part is completed (Fig. 2). Unbound powder is removed, leaving the fabricated part.

Devices consisting PCL and polyethylene oxides (PEO) were fabricated to demonstrate control of drug delivery profiles by controlling the position, composition, and microstructure [26]. The top and bottom layers of the device were constructed by binding PCL power into thin solid layers. A cellular-type pattern was printed with PEO, which has a faster degradation rate, in the intermediate layers. Dyes, which represent drugs, were selectively placed within the cells manually. Control over the release mechanism by controlling device wall composition, anisotropy, and microstructure was achieved with this technique [26].

4.3. Laser stereolithography

Similar to three-dimensional printing but working in a liquid environment, laser stereolithography is a

method that allows real three-dimensional microfabrication [27–29]. A 3D solid model designed with CAD software is numerically sliced into a series of 2D layers with an equal thickness [30]. The code generated from each sliced 2D file is then executed to control a motorized $x-y-z$ platform immersed in a liquid photopolymer. The liquid polymer is selectively exposed to a focused laser light, which moves in $x-y$ directions. The polymer cures and forms a solid in the focal point only. After the first layer is formed the elevator moves downward and a new layer of polymer is solidified according to the design (Fig. 3). This layer-by-layer micro-manufacturing enables complex internal features such as complex passageways and curved surfaces to be accurately produced. Furthermore, by using different proteins and microparticles containing polymer solutions for each layer (or even for partial layers),
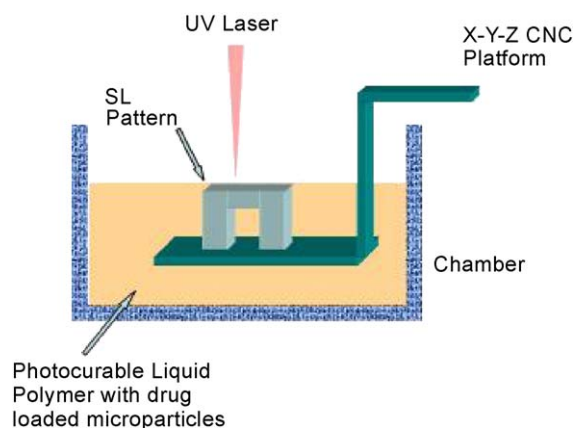
Fig. 3. Schematic setup of a laser stereolithography system.
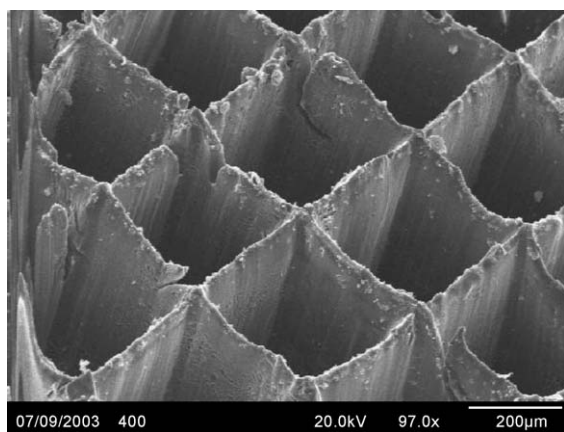
Fig. 4. Cellular-type structure produced by laser stereolithography. Fluorescein microparticles were embedded in PEG-DMA walls. 400 × 400 μm pore size.

we are able to create a precise spatial distribution of biochemical microenvironments.

PLGA (50:50) microparticles encapsulating fluorescein or rhodamine isothiocyanate were used as a model drug containing microparticles [30]. Polyethylene glycol dimethacrylates (PEGDMA, Mw 1000) was mixed with a cyto-compatible photoinitiator (Darocure 2959) along with different microparticles. This mixture was photo-polymerized, layer-by-layer using a frequency tripled Nd:YAG laser (355 nm) and a micromanipulator stage. Different spatial distributions of the microparticles were created and evaluated using a laser scanning confocal microscope to optimize laser energy, initiator concentration, accuracy of spatial distribution, etc.

A cellular structure is shown in Fig. 4. Square pores were formed by solidifying vertical walls with a 400-μm interline spacing. We can also control the spatial distribution of fluorescein and rhodamine microparticles inside a photo-crosslinked polymer layer. A cellular structure containing fluorescein microparticles (1 μm in diameter) and a quadrant structure, with precisely controlled distribution of fluorescein and rhodamine microparticles (5 μm in
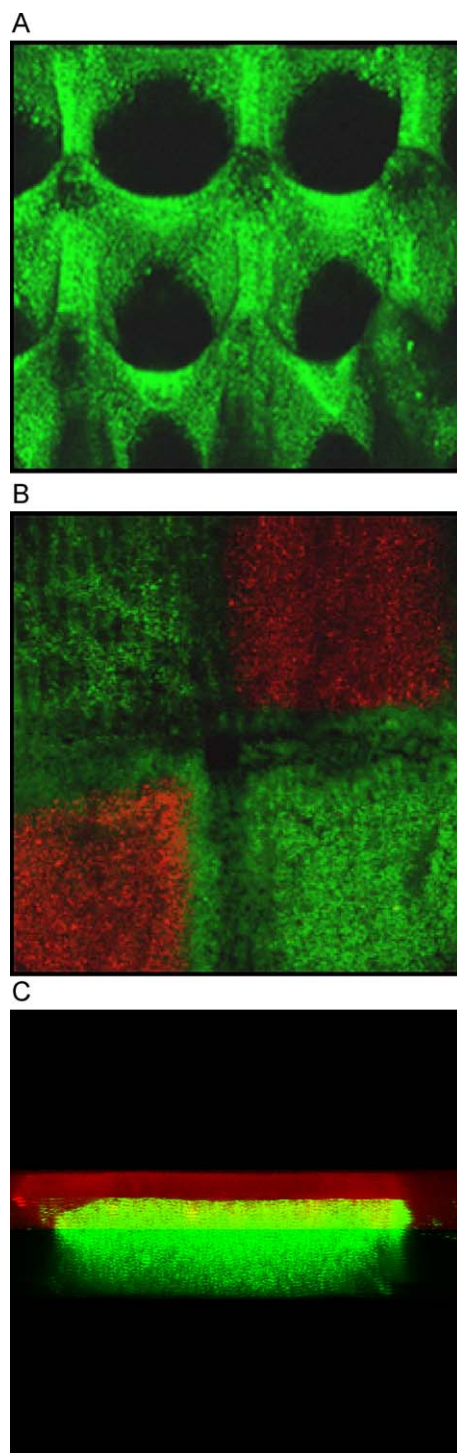
Fig. 5. Confocal fluorescent microscope images of (A) cellular-type structure containing fluorescein microparticles; (B) precise spatial distribution of biodegradable microparticles within photo-polymerized scaffold structures; (C) 3D reconstructed confocal image of a micro-fabricated scaffold structure with spatially patterned fluorescein and rhodamine encapsulated microparticles.

diameter), are shown in Fig. 5A and B. A computer reconstructed cross-section of a particle contained two-layer structure is shown in Fig. 5C. As indicated, precise, pre-designed distributions of controlled release biofactors could be engineered within such scaffold structures [30].

Future work will focus on the functionalization of the PEG macromer with extracellular matrix components to increase cell adhesion and prevent factor diffusion after release. Cell attachment and growth of mesenchymal stem cells (MSCs) will be optimized and followed by attempts to grow hybrid mesenchymal tissue structures (e.g., cartilage and bone or bone and ligaments).

5. Laser micromachining

5.1. Lasers for micropatterning

Laser micromachining makes it possible to pattern polymeric materials on the micro-scale, avoiding the difficulties associated with non-photon techniques. Photons of the laser light act as "clean particles," and the laser irradiation is essentially non-invasive and a single-step process. The most popular lasers used for machining polymers are the UV lasers including excimer, argon-ion, tripled and quadrupled Nd: YAG, fluorine, helium−cadmium, metal vapor, and nitrogen lasers [31]. The small wavelengths allow strong interactions of the beam with a variety of materials. If the incident photon energy is high enough to break the chemical bonds of the target material directly, the material is dissociated into its chemical components and no liquid phase transition occurs. This photochemical process has greatly min-

imized heat effects compared with the photothermal process involved in visible and infrared lasers. This important feature makes UV laser micromachining very attractive for biodegradable polymer materials, since thermal damage to the non-machined part can be minimized. An alternative tool for micromachining polymers is femtosecond solid-state lasers with a near-infrared (NIR) wavelength, ultrashort pulse and high peak power. In polymers, the extremely high intensities generated with femtosecond pulses can produce very high concentrations of free electrons via multi-photon absorption and avalanche ionization. Such strongly non-linear interaction processes can further enhance the localization of the excitation energy, thus increases the resolution in surface patterning [32].

5.2. Laser micropatterning of polymers

We used a variety of lasers to pattern biodegradable polymers [33,34]. The micromachining setup for biodegradable polymer ablation consists of four main parts: a laser system, a beam delivery system, a micrometer-resolution $x−y$ sample stage, and an on-line monitoring system (Fig. 6). The beam delivery system consists of a mask, field lens, turning mirrors and an imaging lens to the beam for micromachining. A spherical lens was used to drill microholes, while a cylindrical lens was used to produce micron-sized channel type patterns. A charge-coupled device (CCD) camera coupled with a TV monitor is used to provide online machining information.

A frequency quadrupled Nd:YAG at 266 nm and a solid-state femtosecond laser at 700 nm (with a Gaussian beam profile) were used to fabricate microhole arrays (Fig. 7). A circular mask was used to
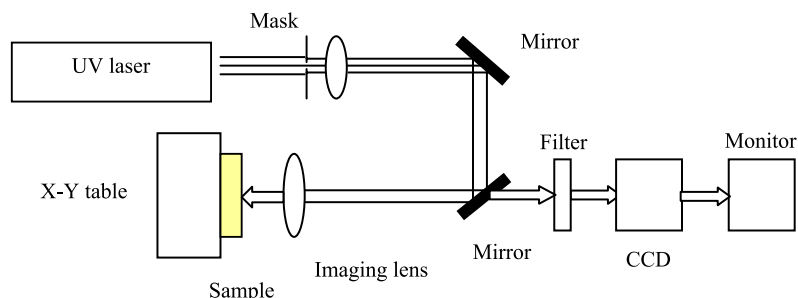
Fig. 6. Schematic setup of a laser micromachining system.
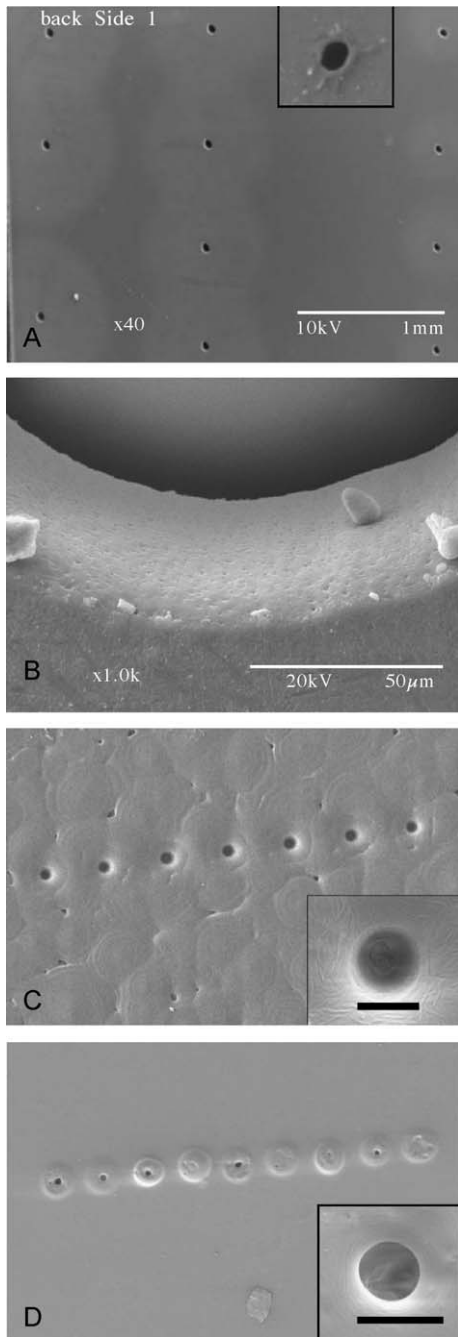
Fig. 7. Laser-drilled microholes in (A) PVA by 266 nm laser; (B) PVA by 193 nm laser; (C) PCL by 700 nm femtosecond laser (10 μm in diameter); (D) PDLA by 700 nm femtosecond laser (8 μm in diameter).
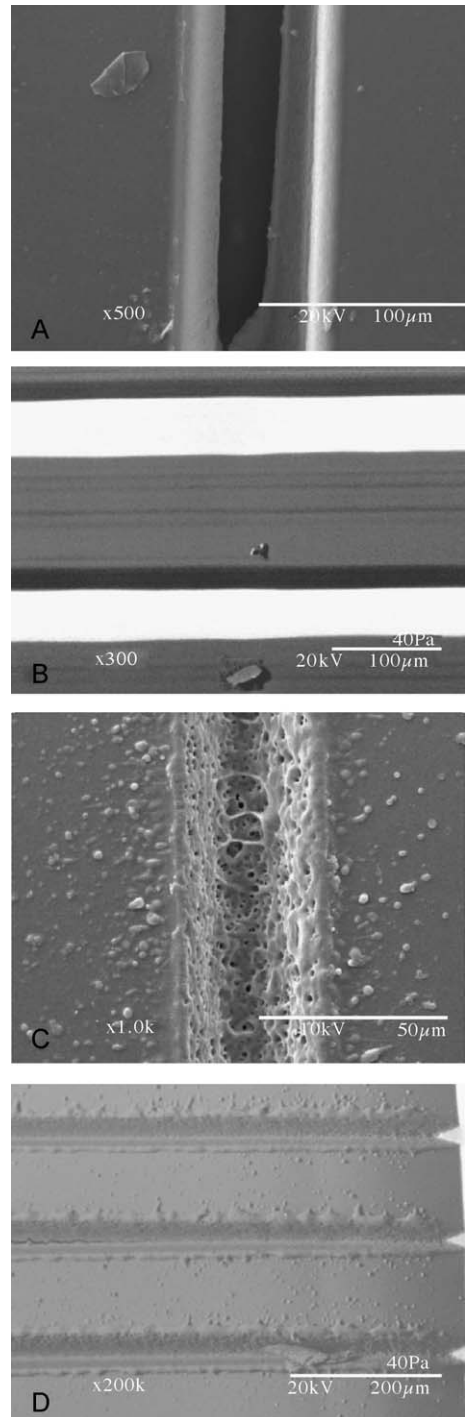
Fig. 8. Laser ablated microchannels in (A) PVA by 193 nm laser; (B) PDLA by 193 nm laser; (C) PVA by 308 nm laser; (D) PDLA by 308 nm laser.

shape the beam. A XeCl excimer laser (308 nm) and an ArF excimer laser (193 nm with a uniform beam profile) were used to irradiate the polymers to fabricate microchannels (Fig. 8). Lenses with 25 and 50 mm focal lengths were used to obtain microchannels with different width grooves. The arrays of holes drilled could be used as degradable microfilters or drug reservoirs while the channels could be used for microfluidic delivery systems. All the experiments were conducted in ambient air. Details of the lasers used in this work are listed in Table 2.

No melting or redeposition was noticed in the case of 193 nm laser (Figs. 7 and 8A,B), while resolidified polymer debris were found around the machined holes and channels at wavelengths of 308 and 266 nm (Figs. 7A and 8C,D). This is because at the 308 nm wavelength, the photon energy of light is only 4.02 eV. This energy is not high enough to break the polymer bonds. At 193 nm wavelength, the photon energy of the laser beam reaches about 7.9 eV, which is well above the bond energies of the polymer. The femtosecond laser delivered a clean cut on the edge of the holes (Fig. 7C,D). The irregularities in the hole shape can be attributed to the spherical aberration and non-circularity of the original laser beam. By using advanced beam delivery systems and beam shapers, the irregularity of the hole shape can be corrected.

Another potential feature of laser ablation is the capability of surface modification of microfabricated structures concurrent with structure formation (e.g., channels) [35]. Many reactive species are formed both at the polymer surface and in the gas phase during the laser ablation process. The incorporation or reaction of these ablation products at the nascent channel walls can result in surface chemical functionality that is significantly different from that in the bulk of the polymer [36]. Incorporation of nitrogen or oxygen can give rise to amino, hydroxyl, carboxylic, or phenolic functional groups at the surface [37]. These types of surface functionalities are thought to play an important role in electroosmotic flow, a commonly used means to pump solution through microchannels [38].

6. Nanosphere lithography

Laser direct patterning provides a resolution on the order of microns due to an optical diffraction limit of the laser wavelength, which is $\lambda/2$ NA, where λ is the wavelength and NA is the numerical aperture of the focusing lens. A typical value of NA in air ranges from 0.5 to 1.0. Therefore, the machining resolution is in the order of λ. In order to achieve nano-scale resolution, near-field photolithographic techniques were developed for nano-structuring by delivering a laser beam through a hollow near-field tip or illuminating the tip of a scanning probe microscope with a pulsed laser [39,40]. A strong local optical field was established between the sample surface and the sharp tip when the surface/tip gap was of a few nanometers. Structures with lateral dimensions below 30 nm, and therefore well below the minimal resolvable feature size of half the wavelength of the light, were produced underneath the tip [41–43]. However, this kind of near-field nanolithographic technique has hardly been used in an industrial setting due to its limited throughput, hollow tip blockage, and difficulty in process control.

We used a new approach involving the illumination of a nanometer-sized sphere array using a laser beam to pattern a solid surface in a mass production fashion [44–46]. A spherical particle may act as a lens and therefore intensifies the incoming laser beam if the sphere diameter is larger than the laser wavelength. Near-field enhancement may play an important role if the diameter of the spherical particle is equal or smaller than the wavelength.

6.1. Sample preparation and processing

PCL thin films with a flat surface (surface roughness in the order of 10 nm) were prepared and used as a substrate for better investigation, even though a flat surface is not required for this process. A 1% (w/v) colloid of silica spheres (diameter = 640 nm) was dropped onto the PCL substrate [47]. Water was then evaporated from the solution in a chamber under a

Table 2
Properties of lasers used in this study

Medium	ArF	Nd:YAG	XeCl	Ti:Sapphire
Wavelength (nm)	193	266	308	700
Pulse energy (mJ)	5	275	300	0.007
Repetition rate (Hz)	10–100	1–10	1–100	15000
Pulse width (ns)	6	6–7	20	0.15

controlled humidity. As the solvent evaporated, capillary forces drew the nanospheres together, and the nanospheres reorganized themselves in a hexagonally close-packed pattern on the substrate (Fig. 9A). The as-deposited nanosphere array may include a variety of defects that arise as a result of nanosphere polydispersity, site randomness, point defects, and line defects.

With a setup similar to that of laser micromachining, samples were irradiated with the second and third harmonic wave of a Nd:YAG laser or a ArF excimer laser. The laser beam was focused by a lens (f = 50.8 mm) onto the sample mounted on a three-dimensional precision stage. All experiments were performed under ambient conditions.

6.2. Nanostructure formation

Most of the spheres in the round shape area exposed to the laser pulse with the diameter of 10 μm disappeared, leaving holes with the same hexagonal pattern as the spheres were formed on the PCL surface (Fig. 9B). A similar phenomenon was observed in Fig. 9C, where spheres at the monolayer edge and adjacent holes were aligned in a hexagonal arrangement, and therefore the spheres located themselves on the holes.

Laser energy was varied from a minimum threshold energy, below which no clear nanostructure was observed, to a maximum energy, beyond which the polymer surface was ablated directly by the laser pulse. In three cases, the diameter of the hole were 430 nm (Fig. 9C), 360 nm (Fig. 9B) and 240 nm (Fig. 9C), corresponding to 355, 266, and 193 nm laser wavelengths, and remained unchanged within the experiment laser energy range. The features were cleaner as the laser wavelength decreased.

The enhanced optical field by nanospheres in the near-field region, which, we believe, produces nano-scale features, can be explained by Mie scattering. When the diameter of the sphere is equal or greater than the wavelength, light is scattered elastically according to the Mie scattering law. The electric field around a Mie sphere (sphere diameter larger than the laser wavelength) is enhanced by several times of the incident light towards the forward area of the sphere [48].

One advantage of this process lies in its simplicity and massively parallel capability for nano-scale sur-
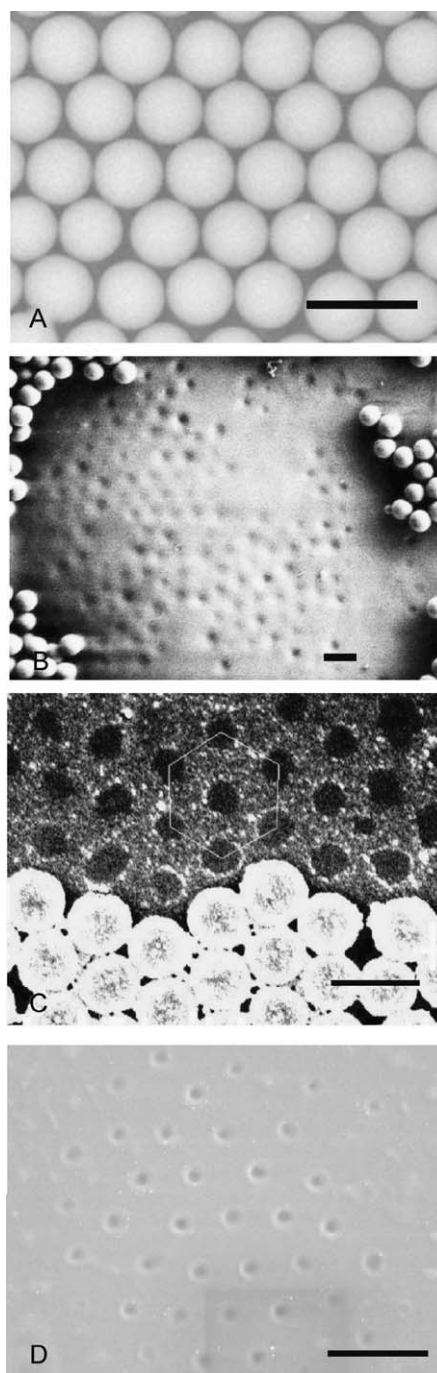
Fig. 9. (A) Self-assembled nanosphere monolayer in close-packed hexagonal form. (B) Nanohole array in PCL by 355 nm laser. Spheres at the monolayer edge and adjacent holes are aligned in a hexagonal arrangement. (C) Nanohole array in PCL by 266 nm laser. (D) Nanohole array in PCL by 193 nm laser.

Table 3
Characteristics of fabrication techniques

Fabrication techniques	Critical dimension	Throughput	Solvent	Feature flexibility	Tool cost
μ-Imprinting lithography	~ 50 nm	high	none	2D structures	master is expensive
Soft lithography	~ 50 nm	high	organic solvent	3D is possible by laminating	soft master is inexpensive
Direct deposition	~ 5 μm	low	organic solvent	simple geometry	tools are simple and inexpensive
Three dimensional printing	~ 50 μm	low	organic solvent	any 3D structures	high-resolution ink-jet system required
Laser stereolithography	~ 10 μm	low	water as solvent	any 3D structures	high-resolution positioning system required
Laser micromachining	~ 1 μm	intermediate	none	2D structures	high-resolution positioning system required
Nanosphere lithography	~ 100 nm	high	none	restricted by self-assembled sphere patterns	cheap

face patterning. Future work is needed on characterizing changes in surface chemical properties in laser processed areas.

7. Summary and future prospects

We summarize the important characteristics of each fabrication technique in Table 3. By employing newly developed fabrication techniques, with manufacturing costs and biocompatibility in mind, we have the unique ability to engineer a micro or nano-scale biomimetic environment. These approaches allow us to study molecular interactions at the cellular level and to control drug delivery. Top–down approaches, some of which are reviewed in this article, provide great flexibility and control of the structures on a micron or submicron scale. The bottom–up approaches, which involve the molecular scale self-assembly, are widely believed to have great potential in terms of fabricating nano-scale devices. We anticipate that the combination of top–down and bottom–up approaches will lead to new technologies in the fabrication of novel drug delivery systems.

Acknowledgements

References

[1] J.T. Santini, A.C. Richards, R. Scheidt, M.J. Cima, R. Langer, Microchips as controlled drug-delivery devices, Angew. Chem., Int. Ed. Engl. 39 (2000) 2396–2407.

[2] T.A. Desai, W.H. Chu, J.K. Tu, G.M. Beattie, A. Hayek, M. Ferrari, Microfabricated immunoisolating biocapsules, Biotechnol. Bioeng. 57 (1998) 118–120.

[3] A. Ahmed, C. Bonner, T.A. Desai, Bioadhesive microdevices with multiple reservoirs: a new platform for oral drug delivery, J. Control. Release 81 (2002) 291–306.

[4] M.L. Reed, C. Wu, J. Kneller, S. Watkins, D.A. Vorp, A. Nadeem, L.E. Weiss, K. Rebello, M. Mescher, A.J.C. Smith, W. Rosenblum, M.D. Feldman, Micromechanical devices for intravascular drug delivery, J. Pharm. Sci. 87 (1998) 1387–1394.

[5] J. Wilbur, A. Kuman, H. Biebuyck, E. Kim, G.M. Whitesides, Microcontact printing of self-assembled monolayers: applications in microfabrication, Nanotechnology 7 (1996) 452–457.

[6] M.S. Widmer, P.K. Gupta, L. Lu, R.K. Meszlenyi, G.R.D. Evans, K. Brandt, T. Savel, A. Gurlek, C.W. Patrick Jr., A.G. Mikos, Manufacture of porous biodegradable polymer conduits by an extrusion process for guided tissue regeneration, Biomaterials 19 (1998) 1945–1955.

[7] A.G. Mikos, Y. Bao, L.G. Cima, D.E. Ingber, J.P. Vacanti, R. Langer, Preparation of poly(glycolic acid) bonded fiber struc-

tures for cell attachment and transplantation, J. Biomed. Mater. Res. 27 (1993) 183–189.

[8] A.G. Mikos, G. Sarakinos, S.M. Leite, J.P. Vacanti, R. Langer, Laminated three-dimensional biodegradable forms for use in tissue engineering, Biomaterials 14 (1993) 323–330.

[9] R. Langer, New methods of drug delivery, Science 249 (1990) 1527–1533.

[10] E. Holy, J.A. Fialkov, J.E. Davies, M.S. Shoichet, Use of a biomimetic strategy to engineer bone, J. Biomed. Mater. Res. Part A 15 (2003) 447–453.

[11] P.X. Ma, R. Zhang, Microtubular architecture of biodegradable polymer scaffolds, J. Biomed. Mater. Res. 15 (2001) 469–477.

[12] D.H. Lewis, in: M. Chasin, R. Langer (Eds.), Biodegradable Polymers as Drug Delivery Systems, vol. 45, Marcel Dekker, New York, 1990, pp. 1–8.

[13] C. Miller, H. Shanks, A. Witt, G. Rutkowski, S. Mallapragada, Oriented Schwann cell growth on micropatterned biodegradable polymer substrates, Biomaterials 22 (2001) 1263–1269.

[14] D.K. Armani, C. Liu, Microfabrication technology for polycaprolactone, a biodegradable polymer, J. Micromechanics Microengineering 10 (2000) 80–84.

[15] C.G. Pitt, Poly-caprolactone and its copolymers, in: M. Chasin, R. Langer (Eds.), Biodegradable Polymers as Drug Delivery Systems, vol. 45, Marcel Dekker, New York, 1990, pp. 71–119.

[16] S.Y. Chou, P.R. Krauss, P.J. Renstrom, Imprint of sub-25 nm vias and trenches in polymers, Appl. Phys. Lett. 67 (1995) 3114–3116.

[17] H.W. Lehmann, R. Widmer, M. Ebnoether, A. Wokaun, M. Meier, S.K. Miller, Fabrication of submicron crossed square wave gratings by dry etching and thermoplastic replication techniques, J. Vac. Sci. Technol., B 1 (1983) 1207–1210.

[18] F. Gottschalch, T. Hoffmann, C.M.S. Torres, H. Schulzb, H.-C. Scheer, Polymer issues in nanoimprinting technique, Solid-State Electron. 43 (1999) 1079–1083.

[19] N. Patel, R. Padera, G.H.W. Sanders, S.M. Cannizzaro, M.C. Davies, R. Langer, C.J. Roberts, S.J.B. Tendler, P.M. Williams, K.M. Shakessheff, Spatially controlled cell engineering on biodegradable polymer surfaces, FASEB 12 (1998) 1447–1454.

[20] C.S. Chen, M. Mrksich, S. Huang, G.M. Whitesides, D.E. Ingber, Geometric control of cell life and death, Science 176 (1997) 1425–1428.

[21] Y.N. Xia, G.M. Whitesides, Soft lithography, Annu. Rev. Mater. Sci. 28 (1998) 153–184.

[22] R. Landers, R. Mühaupt, Desktop manufacturing of complex objects, prototypes and biomedical scaffolds by means of computer-assisted design combined with computer-guided 3D plotting of polymers and reactive oligomers, Macromol. Mater. Eng. 282 (2000) 17–31.

[23] G. Vozzi, C. Flaim, A. Ahluwalia, S. Bhatia, Fabrication of PLGA scaffolds using soft lithography and microsyringe deposition, Biomaterials 24 (2003) 2533–2540.

[24] I. Zein, D.W. Hutmacher, K.C. Tan, S.H. Teoh, Fused deposition modeling of novel scaffold architectures for tissue engineering applications, Biomaterials 23 (2003) 1169–1185.

[25] N.K. Vail, J.W. Barlow, J.J. Beaman, H.L. Marcus, D.L. Bourell, Development of a poly(methyl methacrylate-co-n-butyl methacrylate) copolymer binder system, J. Appl. Polym. Sci. 9 (1994) 789–812.

[26] B.M. Wu, S.W. Borland, R.A. Giordano, L.G. Cima, E.M. Sachs, M.J. Cima, Solid free-form fabrication of drug delivery devices, J. Control. Release 40 (1996) 77–87.

[27] T. Hagiwara, Recent progress of photo-resin for rapid prototyping "resin for stereolithography", Macromol. Symp. 175 (2001) 397–402.

[28] M.N. Cooke, J.P. Fisher, D. Dean, C. Rimnac, A.G. Mikos, Use of stereolithography to manufacture critical-sized 3D biodegradable scaffolds for bone ingrowth, J. Biomed. Mater. Res. Part B: Appl Biomater. 64B (2002) 65–69.

[29] T. Matsuda, M. Mizutani, S.C. Arnold, Molecular design of photocurable liquid biodegradable copolymers. Synthesis and photocuring characteristics, Macromolecules 33 (2000) 795–800.

[30] Y. Lu, G. Mapili, S.C. Chen, K. Roy, Spatio-temporal patterning of growth factors in micro-fabricated scaffolds, 30th Annual Meeting and Exposition, Glasgow, Scotland, 2003.

[31] R.C. Crafer, P.J. Oakley, Laser Processing in Manufacturing, Chapman & Hall, New York, 1993, pp. 1–20.

[32] D. Bäuerle, Laser Processing and Chemistry, Springer, New York, 2000, pp. 259–281.

[33] V. Kancharla, S.C. Chen, Fabrication of biodegradable polymeric micro-devices using laser micromachining, Biomed. Microdev. 4 (2002) 105–109.

[34] S.C. Chen, V. Kancharla, Y. Lu, Laser-based microscale patterning of biodegradable polymers for biomedical applications, Int. J. Mater. Prod. Technol. 18 (2003) 457–468.

[35] P. Laurens, M. Ould Bouali, F. Meducin, B. Sadras, Characterization of modifications of polymer surfaces after excimer laser treatments below the ablation threshold, Appl. Surf. Sci. 154–155 (2000) 211–216.

[36] D. Knittel, E. Schollmeyer, Surface structuring of synthetic polymers by UV-laser irradiation: Part IV. Applications of excimer laser induced surface modification of textile materials, Polym. Int. 45 (1998) 110–117.

[37] M.A. Roberts, J.S. Rossier, P. Bercier, H. Girault, UV laser machined polymer substrates for the development of microdiagnostic systems, Anal. Chem. 69 (1997) 2035–2042.

[38] S.L.R. Barker, D. Ross, M.J. Tarlov, M. Gaitan, L.E. Locascio, Control of flow direction in microfluidic devices with polyelectrolyte multilayers, Anal. Chem. 72 (2000) 5925–5929.

[39] E. Betzig, J.K. Trautman, Near-field optics: microscopy, spectroscopy, and surface modification beyond the diffraction limit, Science 257 (1992) 189–195.

[40] M. Ohtsu, H. Hori, Near-Field Nano-Optics, Kluwer Academic Publishing, New York, 1999, pp. 1–10.

[41] Y.F. Lu, Z.H. Mai, G. Qiu, W.K. Chim, Laser-induced nano-oxidation on hydrogen-passivated Ge (100) surfaces under a scanning tunneling microscope tip, Appl. Phys. Lett. 75 (1999) 2359–2361.

[42] S.M. Huang, M.H. Hong, Y.F. Lu, B.S. Luk'yanchuk, W.D. Song, T.C. Chong, Pulsed-laser assisted nanopatterning of metallic layers combined with atomic force microscopy, J. Appl. Phys. 91 (2002) 3268–3274.

[43] J.A. DeAro, R. Gupta, A.J. Heeger, S.K. Buratto, Nanoscale oxidative patterning and manipulation of conjugated polymer thin films, Synth. Met. 102 (1999) 865–868.

[44] Y. Lu, S. Theppakuttai, S.C. Chen, Marangoni effect in nanosphere-enhanced laser nanopatterning of silicon, Appl. Phys. Lett. 82 (2003) 4143–4145.

[45] Y. Lu, S.C. Chen, Nanopatterning of a silicon surface by near-field enhanced laser irradiation, Nanotechnology 14 (2003) 505–508.

[46] S. Theppakuttai, S.C. Chen, Nanoscale surface modification of glass using a 1064 nm pulsed laser, Appl. Phys. Lett. 83 (2003) 758–760.

[47] R. Micheletto, H. Fukuda, M. Ohtsu, A simple method for the production of a two-dimensional, ordered arrays of small latex particles, Langmuir 11 (1995) 3333–3336.

[48] O. Watanabe, T. Ikawa, M. Hasegawa, M. Tsuchimori, Y. Kawata, Nanofabrication induced by near-field exposure from a nanosecond laser pulse, Appl. Phys. Lett. 79 (2001) 1366–1368.